Tailoring the electronic structure of FeRu-NC for efficient electrochemical oxidative dehydrogenation of L-ascorbic acid

Bing Liu[1,a], Haoming Zhong[1,a], Hina Gul[a], Hao Peng[a,c], Xiaolei Guo[a,b,*], Yu-Long Xie[d], Minhua Ai[a,c], Xiangwen Zhang[a,c], Ji-Jun Zou[a,c], Lun Pan[a,c,*]

[a] Key Laboratory for Green Chemical Technology of the Ministry of Education, School of Chemical Engineering and Technology, National Industry-Education Platform for Energy Storage, Tianjin University, Tianjin 300072, China.

[b] School of Chemical Engineering and Technology, Hebei University of Technology, Tianjin 300401, China.

[c] TJU Binhai Industrial Research Institute Co., Ltd., Tianjin 300452, China.

[d] School of Chemistry and Materials Science, Qinghai Minzu University, Xining 810007, China.

[1] The authors contributed to this work equally.

[*]E-mail: xlguo@hebut.edu.cn (X. Guo); panlun76@tju.edu.cn (L. Pan).

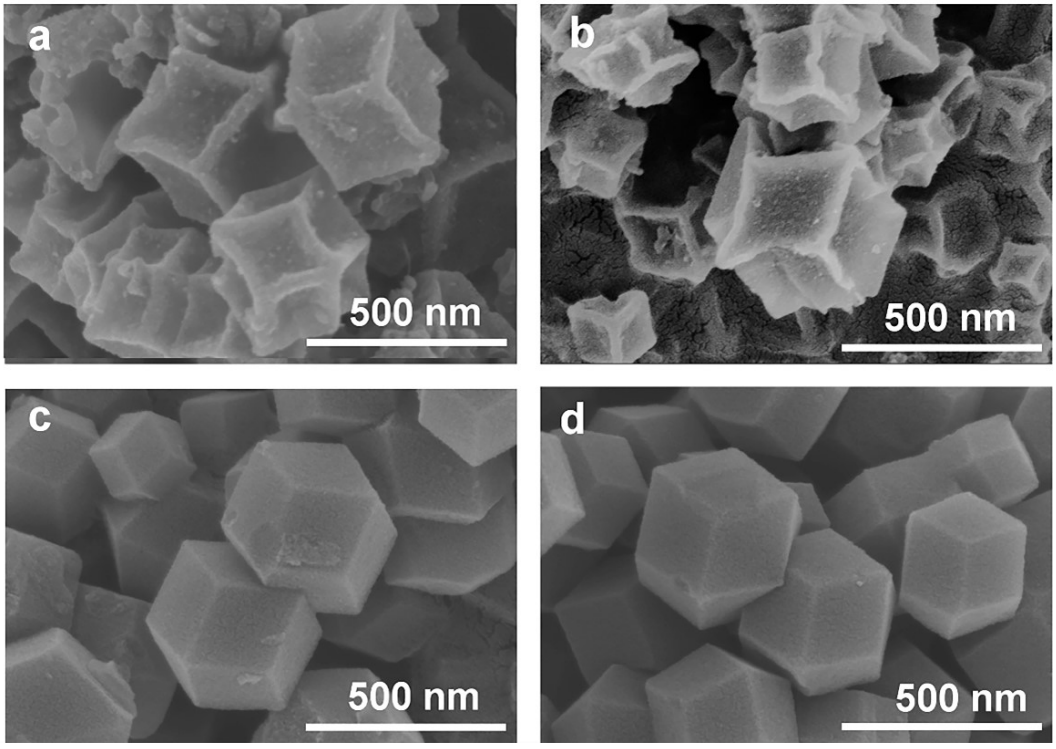

Figure S1. SEM images of (a) FeRu-NC, (b) Fe-NC, (c) Ru-NC, (d) NC.

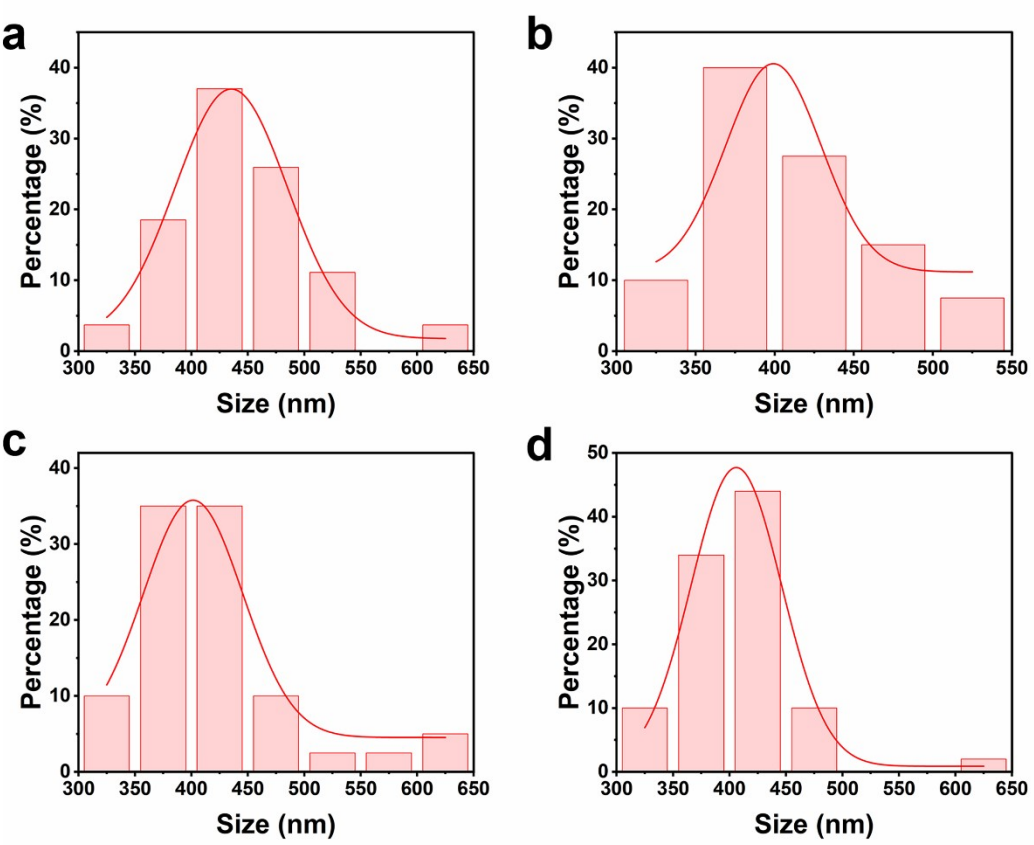

Figure S2. Particle size distribution of (a) FeRu-NC, (b) Fe-NC, (c) Ru-NC, (d) NC.

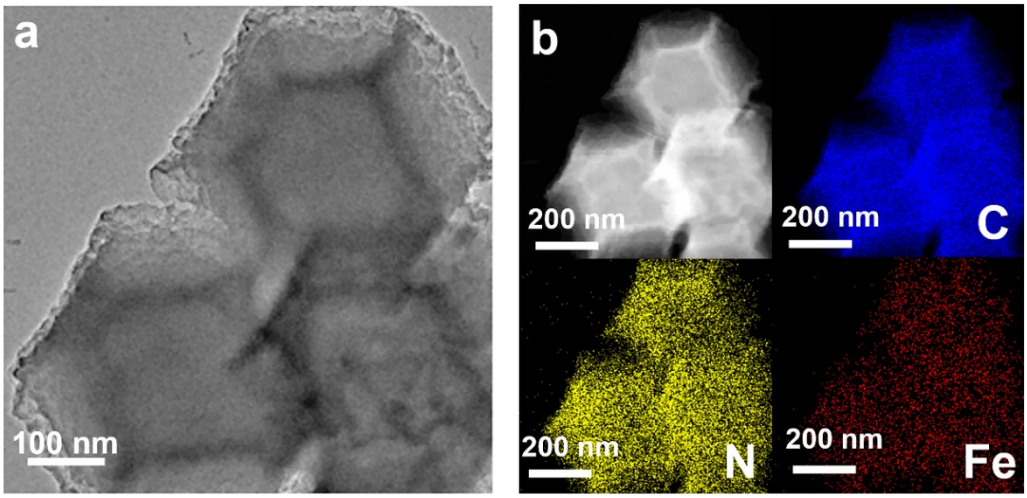

Figure S3. (a) TEM images of Fe-NC. (b) STEM and EDS mapping images of Fe-NC.

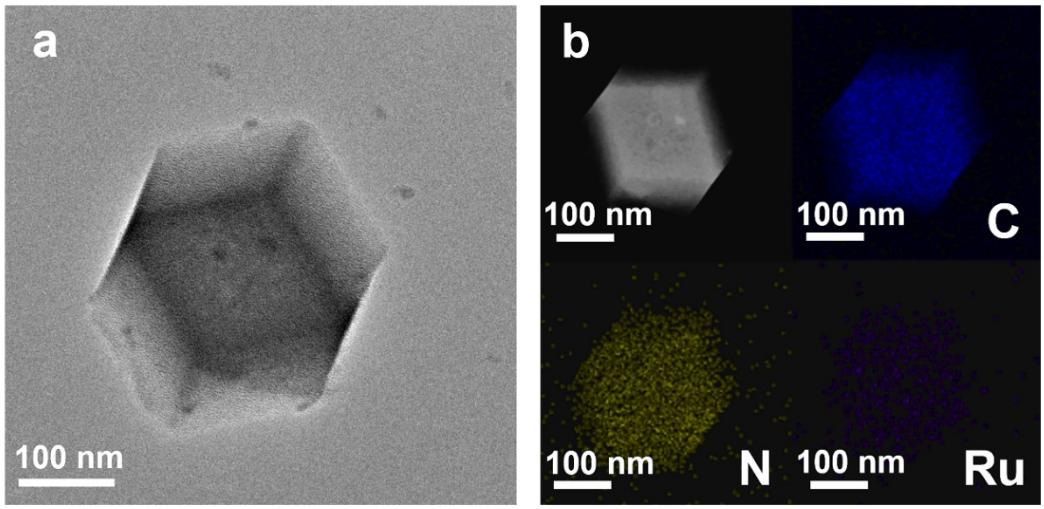

Figure S4. (a) TEM images of Ru-NC. (b) STEM and EDS mapping images of Ru-NC.

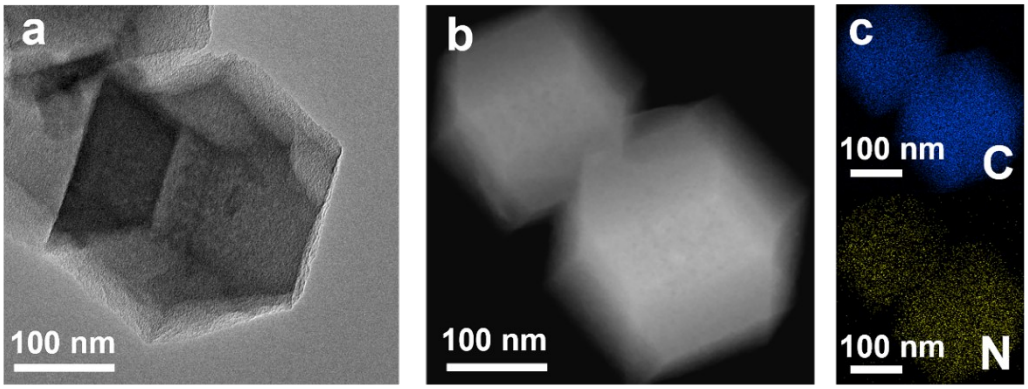

Figure S5. (a) TEM images of NC. (b) STEM images of NC. (c) EDS mapping images of NC.

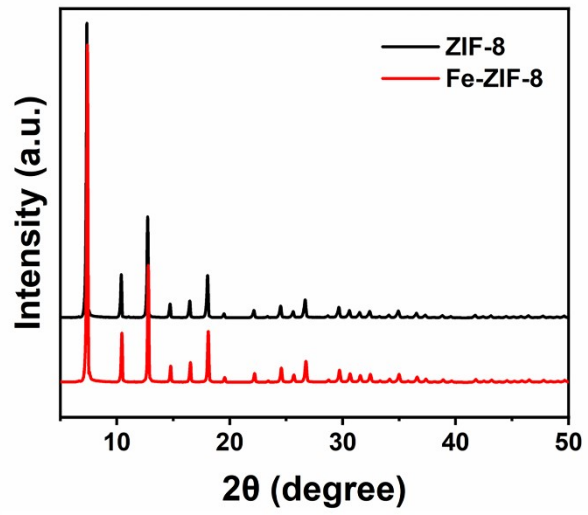

Figure S6. XRD patterns of ZIF-8 and Fe-ZIF-8.

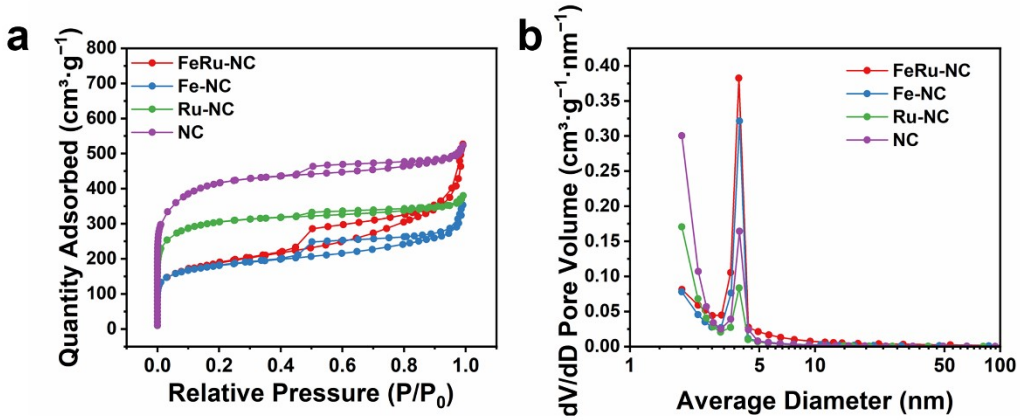

Figure S7. (a) Nitrogen adsorption-desorption isotherms and (b) Pore size distributions of FeRu-NC, Fe-NC, Ru-NC and NC.

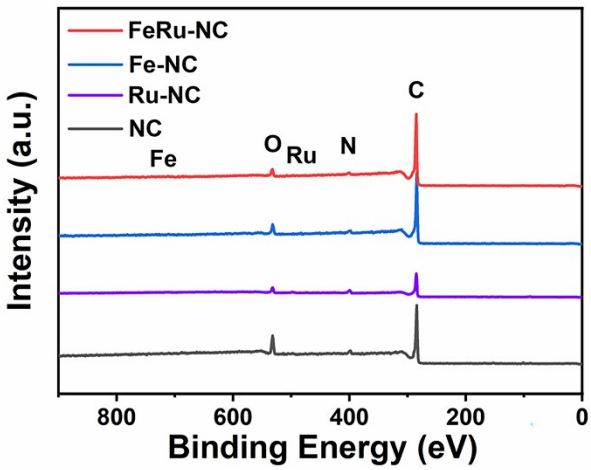

Figure S8. XPS spectra of FeRu-NC, Fe-NC, Ru-NC and NC.

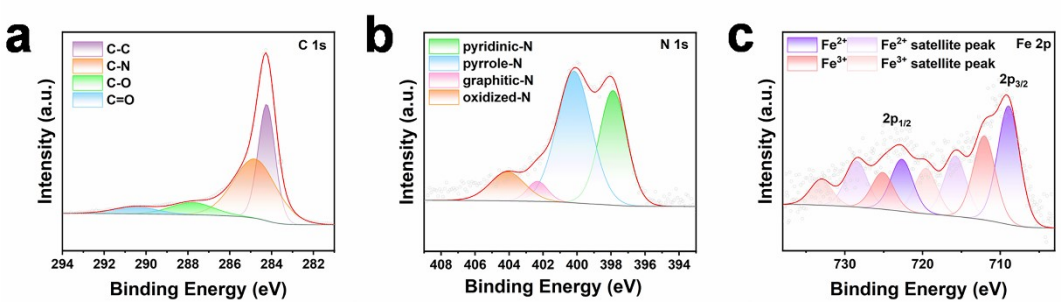

Figure S9. High-resolution XPS spectra of Fe-NC. (a) C 1s XPS spectrum. (b) N 1s XPS spectrum. (c) Fe 2p XPS spectrum.

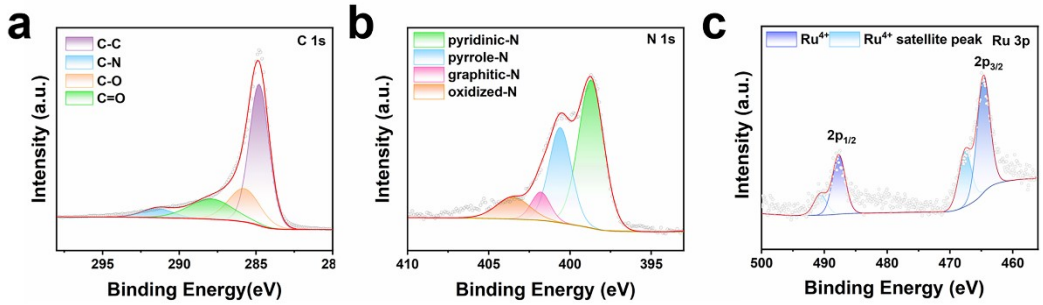

Figure S10. High-resolution XPS spectra of Ru-NC. (a) C 1s XPS spectrum. (b) N 1s XPS spectrum. (c) Ru 3p XPS spectrum.

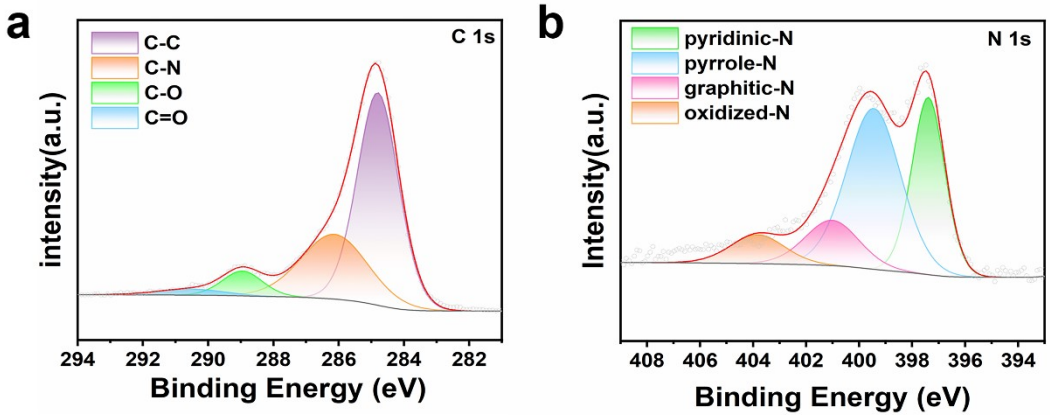

Figure S11. High-resolution XPS spectra of NC. (a) C 1s XPS spectrum. (b) N 1s XPS spectrum.

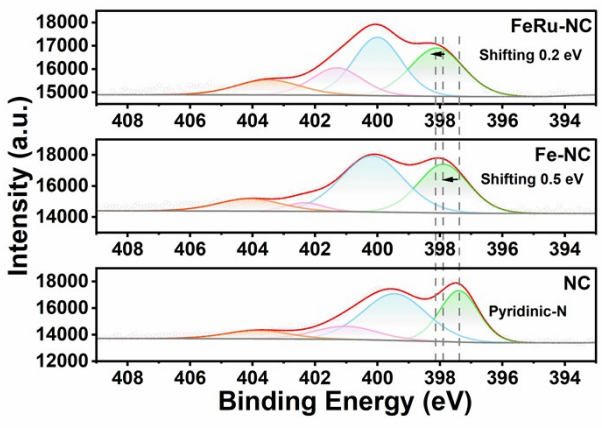

Figure S12. Comparison of N 1s XPS spectra of FeRu-NC, Fe-NC and NC.

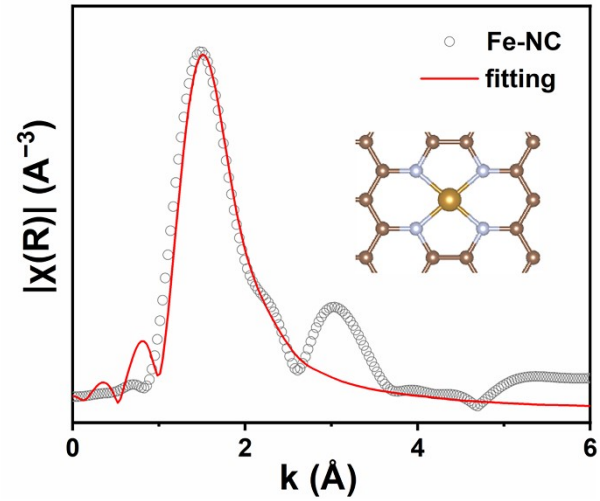

Figure S13. R-space FT-EXAFS fitting plot for Fe-NC.

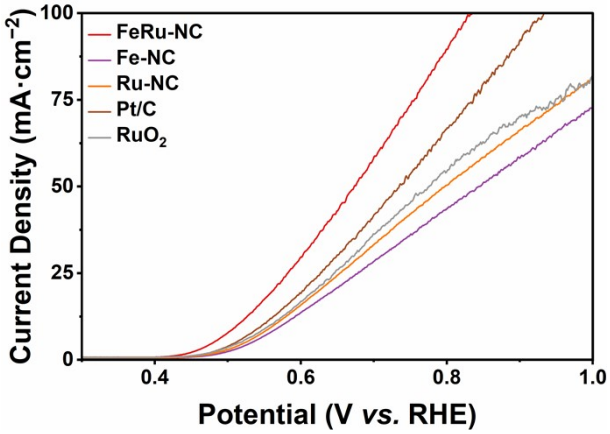

Figure S14. Geometric area-normalized LSV curves without iR compensation.

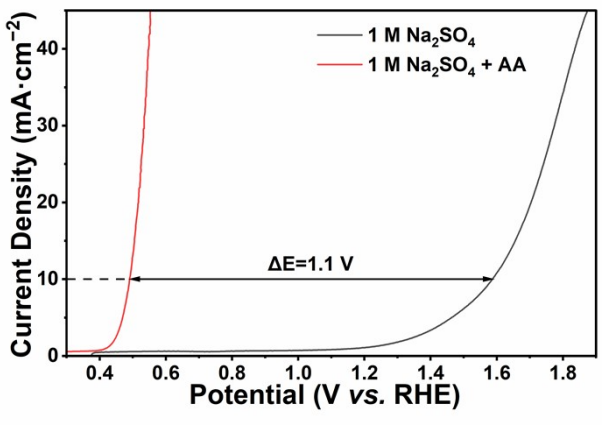

Figure S15. Comparison of LSV curves for FeRu-NC in electrolytes with and without (AA) at pH = 2.3.

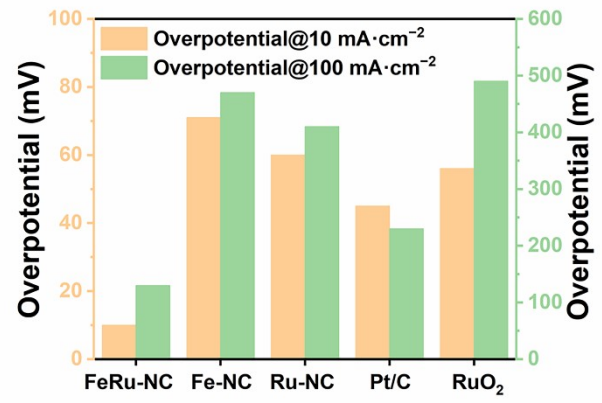

Figure S16. Overpotential comparison for different electrocatalysts, recorded at current densities of 10 mA·cm^{-2} and 100 mA·cm^{-2}.

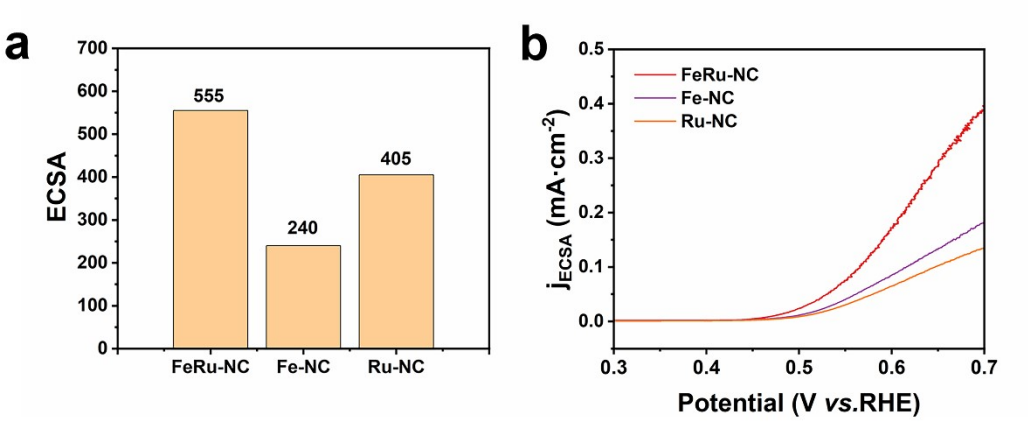

Figure S17. (a) ECSA of FeRu-NC, Fe-NC and Ru-NC. (b) LSV curves with current density normalized by ECSA.

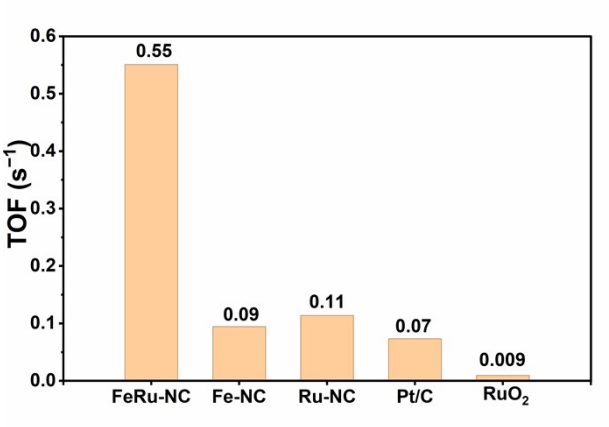

Figure S18. TOF values of FeRu-NC, Fe-NC, Ru-NC, Pt/C and RuO_2.

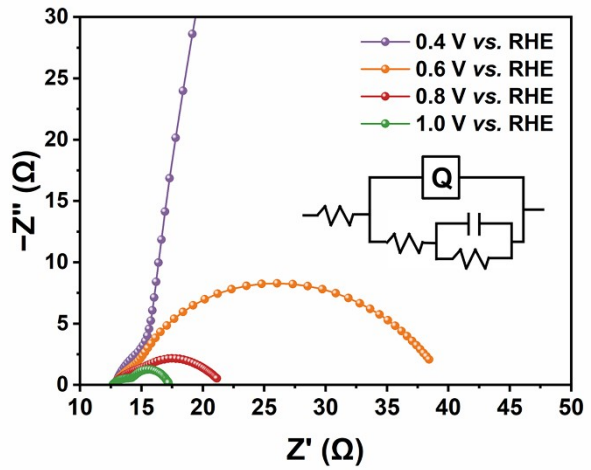

Figure S19. Nyquist plots of FeRu-NC at different potentials.

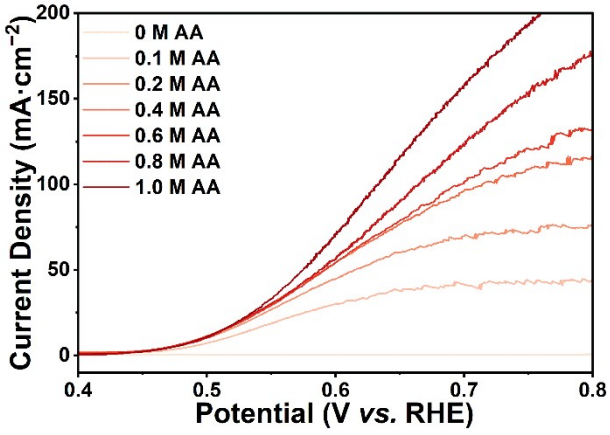

Figure S20. LSV curves (90% IR compensation) of FeRu-NC at different AA concentrations.

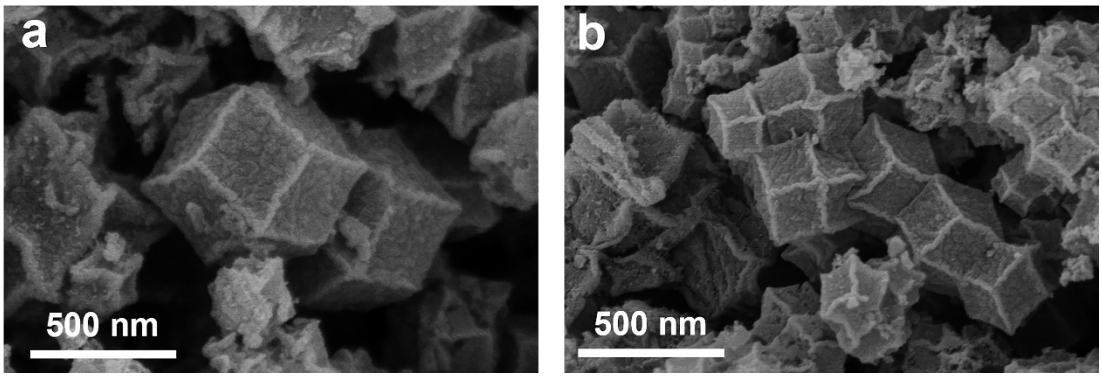

Figure S21. (a, b) SEM images of FeRu-NC after stability test.

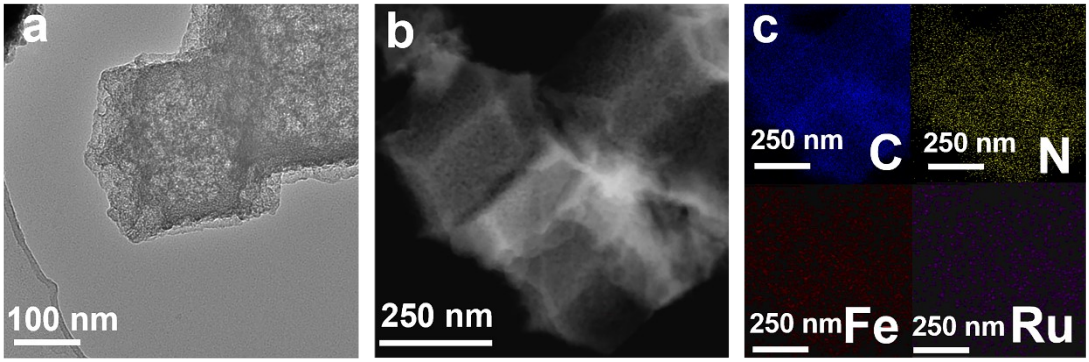

Figure S22. (a) TEM, (b)STEM and (c) EDS mapping images of FeRu-NC after stability test.

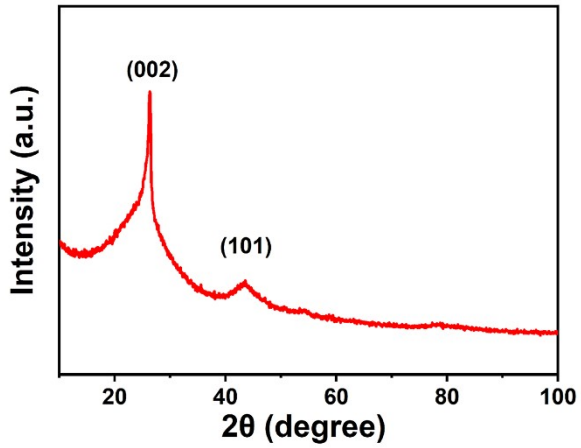

Figure S23. XRD pattern of FeRu-NC after stability test.

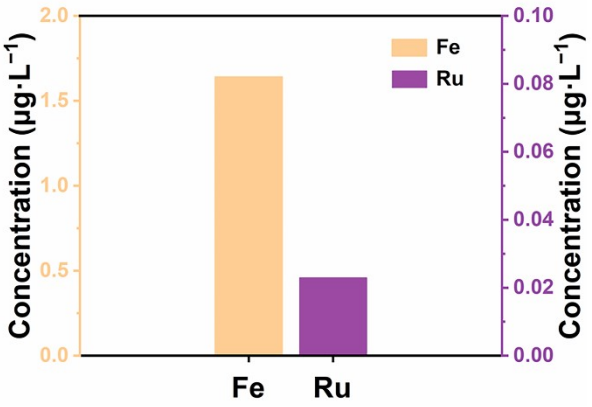

Figure S24. Metal content in the electrolyte after stability test.

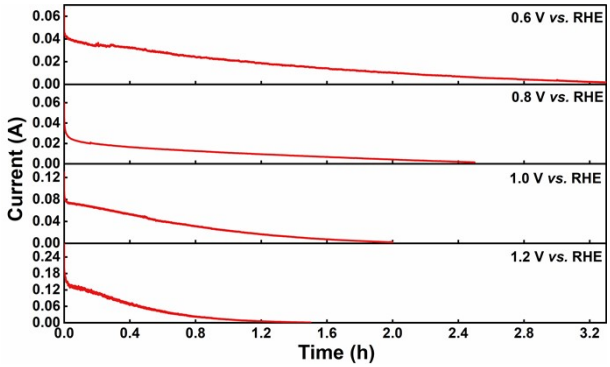

Figure S25. Chronoamperometric tests at different applied potentials.

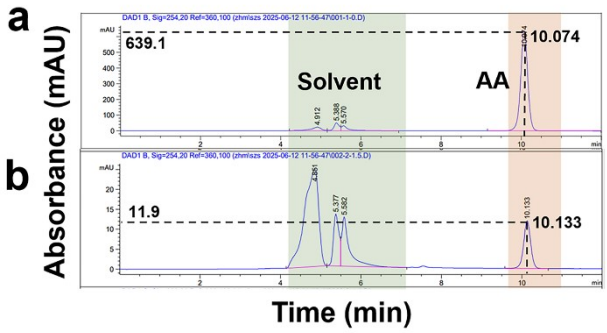

Figure S26. HPLC of electrolyte (a) before and (b) after AAOR.

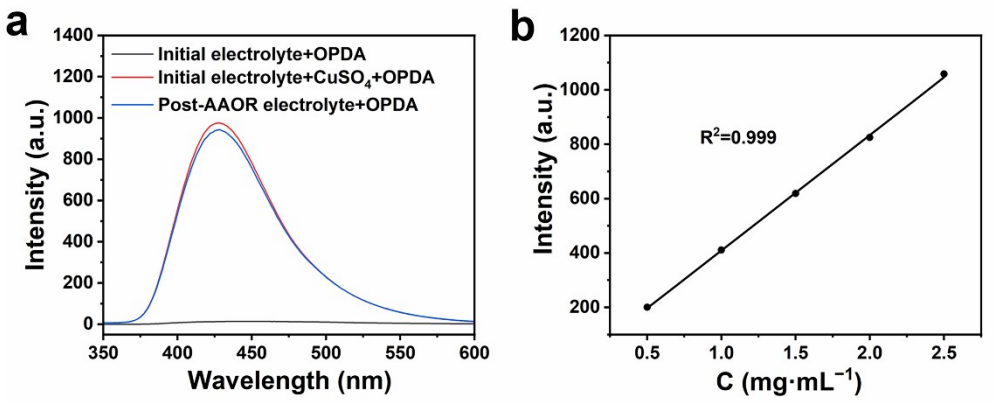

Figure S27. (a) Fluorescence spectra from the reaction of OPDA with the initial electrolyte, the $CuSO_4$-oxidized electrolyte, and the post-AAOR electrolyte. (b) Standard calibration curve for fluorescence spectroscopy.

Table S1. Elemental mass fraction measured by ICP-OES.

	Fe (wt. %)	Ru (wt. %)
FeRu-NC	2.08	0.16
Fe-NC	2.55	/
Ru-NC	/	0.15

Table S2. The surface area and pore size of FeRu-NC, Fe-NC, Ru-NC and NC.

	Surface area ($m^2 \cdot g^{-1}$)	**Pore size (nm)**
FeRu-NC	659	6.1
Fe-NC	646	5.0
Ru-NC	1114	3.3
NC	1508	3.1

Table S3. Elemental quantification of different catalysts determined by XPS.

	Fe (at. %)	**Ru (at. %)**	**C (at. %)**	**N (at. %)**	**O (at. %)**
FeRu-NC	2.47	0.36	90.71	1.29	5.17
Fe-NC	1.77	/	88.19	2.91	7.13
Ru-NC	/	0.65	81.22	8.79	9.35
NC	/	/	82.03	4.88	13.09

Table S4. Content of different N species in FeRu-NC, Fe-NC, Ru-NC and NC.

	pyridinic N (at. %)	**pyrrolic N (at. %)**	**graphitic N (at. %)**	**oxidized N (at. %)**
FeRu-NC	34.61	49.70	4.51	11.17
Fe-NC	33.30	36.30	17.85	12.54
Ru-NC	52.42	29.84	7.45	10.28

NC	31.38	46.89	13.26	8.47

Table S5. Fe peak area ratio of FeRu-NC and Fe-NC determined by XPS.

	Fe^{2+}/Fe^{3+}
FeRu-NC	1.25
Fe-NC	1.37

Table S6. Fe K-edge EXAFS curve fitting parameters.

	Path	**CN**	**R (Å)**	**$\sigma^2\times10^3$ (Å^2)**	**R factor (%)**
FeRu-NC	Fe-N	4.0	2.30	0.31	0.020
Fe-NC	Fe-N	4.0	2.22	0.54	0.018

Table S7. Comparison of the electrocatalytic activity for different biomass oxidation catalysts.

Electrocatalyst	**Biomass additive**	**J ($mA\cdot cm^{-2}$)**	**Potential (V)**	**Ref.**
Fe-Ni_2P@C/NF	arabinose	100	1.36	1
$NiFeO_x$-NF	glucose	100	1.39	2
Fe-Ni_3S_2@NiFe-PBA/NF	HMF	100	1.50	3
$Fe(OH)_x$@$Co_{0.8}Fe_{0.2}$-MOF/NF	HMF	100	1.49	4
Fe-CoP@NC	HMF	100	1.55	5
$(Fe_xCo_{1-x})_4N$-0.9	HMF	100	1.54	6
Fe-CuO_x/CF	glycerol	100	1.33	7
CuFeCoOOH	glycerol	100	1.36	8
PtFe DAC	benzyl alcohol	100	1.28	9
Fe-NF-500	methanol	100	1.38	10
NiFe-LDH	methanol	100	1.41	11
P_O-XC 72	AA	100	0.65	12
FeRu-NC	AA	100	0.61	This work

Table S8. Comparison of overpotential of different electrocatalysts.

	Overpotential@10 $mA\cdot cm^{-2}$	**Overpotential @100 $mA\cdot cm^{-2}$**	**Overpotential @200 $mA\cdot cm^{-2}$**
FeRu-NC	**10**	**130**	**200**
Fe-NC	71	470	/
Ru-NC	60	410	/

Pt/C	45	230	420
RuO_2	56	490	/

Table S9. Fitting parameters from the EIS Nyquist plots of different electrocatalysts.

Electrocatalyst	R_s (Ω)	Q (s^n)	n	R (Ω)	C (F)	R_{ct} (Ω)
FeRu-NC	12.65	0.018	0.53	6.16	0.013	2.85
Fe-NC	12.67	0.006	0.51	3.98	0.053	16.41
Ru-NC	12.54	0.011	0.41	6.96	0.007	15.84
Pt/C	12.40	0.015	0.38	9.77	0.0002	5.62
RuO_2	13.55	0.013	0.58	7.33	0.100	3.55

Table S10. Standard calibration curve parameters for fluorescent micrometer.

Std. No.	Measured value	Concentration (mg·mL^{-1})	diff	RD	t
1	200.39	0.5	0.2	1.34	1.06
2	410.89	1.0	0.1	1.12	−0.78
3	618.50	1.5	−0.2	1.16	0.80
4	824.57	2.0	−0.3	1.81	−1.26
5	1058.26	2.5	0.4	2.45	0.17
AA	701.73	1.7	/	/	/
DHA-0.6 V	495.34	1.2	/	/	/
DHA-0.8 V	619.17	1.5	/	/	/
DHA-1.0 V	635.68	1.54	/	/	/
DHA-1.2 V	681.09	1.65	/	/	/

Table S11. Conversion, selectivity, yield and FE at different potentials.

Potential (V)	Conversion (%)	Selectivity (%)	Yield (%)	FE (%)
0.6	92.37	70.58	65.19	72.75
0.8	93.72	88.23	82.69	87.37
1.0	98.83	90.58	89.53	91.79
1.2	98.15	97.06	95.26	95.46

References

1 D Li, Z. Li, R. Zou, G. Shi, Y. Huang, W. Yang, W. Yang, C. Liu and X. Peng, *Appl. Catal. B-Environ.*, 2022, **307**, 121170.

2 W. J. Liu, Z. Xu, D. Zhao, X. Q. Pan, H. C. Li, X. Hu, Z. Y. Fan, W. K. Wang, G. H. Zhao, S. Jin, G. W. Huber and H. Q. Yu, *Nat. Commun.*, 2020, **11**, 265.

3 N. Li, H. H. Wang, H. Chen, Z. Z. Liu, G. K. Wu, Q. Yang, S. F. Qin, L. X. You and Y. X. Jiang,

Electrochim. Acta, 2024, **495**, 144495.

4 M. Nozari-Asbemarz, S. Arshi, B. Babaei, I. Pisano, E. Magner and J. J. Leahy, *Nanoscale*, 2025, **17**, 8824-8835.

5 M. Qiu, Y. Xiong, W. Zhao, D. Ouyang, Z. Wu, T. Liang, C. Chen, S. Hu and H. Sun, *J. Environ. Chem. Eng.*, 2025, **13**, 117874.

6 L. Wang, Z. Wang, L. Chu, M. Yang and G. Wang, *Electrochim. Acta*, 2024, **492**, 144362.

7 S. Zhong, B. He, S. Wei, R. Wang, R. Zhang and R. Liu, *Appl. Catal. B-Environ.*, 2025, **362**, 124743.

8 Y. Wang, Y. Liu, H. Cai, D. Cao and S. N. Lou, *Small*, 2025, **21**, e06367.

9 G. Song, W. Sun, X. Wang, S. Gong and Y. Tian, *Nano Res.*, 2025, **18**, 94907362.

10 Y. Hao, D. Yu, S. Zhu, C. H. Kuo, Y. M. Chang, L. Wang, H. Y. Chen, M. Shao and S. Peng, *Energy Environ. Sci.*, 2023, **16**, 1100-1110.

11 B. Zhu, B. Dong, F. Wang, Q. Yang, Y. He, C. Zhang, P. Jin and L. Feng, *Nat. Commun.*, 2023, **14**, 1686.

12 B. Zhou, J. Shi, Y. Jiang, L. Xiao, Y. Lu, F. Dong, C. Chen, T. Wang, S. Wang and Y. Zou, *Chin. J. Catal.*, 2023, **50**, 372-380.